AJNR

MR anatomy of the substantia innominata and findings in Alzheimer disease: a preliminary report.

M Sasaki, S Ehara, Y Tamakawa, S Takahashi, H Tohgi, A Sakai and T Mita

AJNR Am J Neuroradiol 1995, 16 (10) 2001-2007
http://www.ajnr.org/content/16/10/2001

MR Anatomy of the Substantia Innominata and Findings in Alzheimer Disease: A Preliminary Report

Makoto Sasaki, Shigeru Ehara, Yoshiharu Tamakawa, Satoshi Takahashi, Hideo Tohgi, Akio Sakai, and Toshio Mita

PURPOSE: To demonstrate normal MR anatomy of the substantia innominata and its changes in Alzheimer disease on MR imaging. **METHODS:** Using a 1.5-T superconductive MR unit, thickness of the substantia innominata was measured on coronal thin-section images obtained in 22 patients with Alzheimer disease and 14 age-matched control subjects. Comparison of these images with postmortem specimens of human brain was also performed. **RESULTS:** On T2-weighted images through the anterior commissure, the substantia innominata was clearly identified between the globus pallidus and the anterior perforated substance. In Alzheimer disease, thinning of the substantia innominata was more frequently observed than in the age-matched controls. **CONCLUSION:** Thin-section T2-weighted coronal MR images can demonstrate shrinkage of the substantia innominata, a finding that may aid in the diagnosis of Alzheimer disease.

Index terms: Brain, anatomy; Brain, magnetic resonance; Dementia; Prosencephalon

AJNR Am J Neuroradiol 16:2001–2007, November 1995

The substantia innominata, in which the nucleus basalis of Meynert exists, is reported to be one of the vulnerable sites in Alzheimer disease (1, 2). Histologic evaluation has shown neuronal loss in the nucleus basalis of Meynert in Alzheimer disease (1, 2). However, on imaging studies the substantia innominata has been a difficult site to evaluate because of its small size. The purposes of our study are twofold: one is to clarify the complex anatomy of the basal forebrain using magnetic resonance (MR) imaging, and the other is to investigate changes of the substantia innominata in patients with Alzheimer disease.

Received October 18, 1994; accepted after revision June 20, 1995.

From the Center for Radiological Sciences (M.S., S.E., Y.T.), Department of Neurology (S.T., H.T.), and Department of Psychiatry (A.S., T.M.), Iwate Medical University, Morioka, Japan.

Supported by a Grant for Scientific Research from the Japanese Ministry of Health and Welfare 1991–1993.

Presented in part at the 79th Scientific Assembly and Annual Meeting of Radiological Society of North America, Chicago, Ill, December 2, 1993.

Address reprint requests to Makoto Sasaki, MD, Center for Radiological Sciences, Iwate Medical University, Uchimaru 19-1, Morioka 020, Japan.

AJNR 16:2001–2007, Nov 1995 0195-6108/95/1610–2001

Anatomy

The basal forebrain in the posterior part of the rhinencephalon consists of several paleopallial structures, including the substantia innominata, the diagonal gyrus, and the paraterminal gyrus (3–7). The substantia innominata and the diagonal gyrus are distributed linearly in the posterior half of the anterior perforated substance. The paraterminal gyrus is located on the medial aspect of the diagonal gyrus and posterior to the subcallosal area (Fig 1A). The characteristic features of the basal forebrain are the existence of aggregations of large cholinergic neurons, such as the nucleus basalis of Meynert in the substantia innominata, the nucleus of the diagonal band of Broca in the diagonal gyrus, and the medial and lateral septal nuclei in the paraterminal gyrus (8–10). There are cholinergic projections from the nucleus basalis of Meynert to the cerebral cortex and from the nucleus of the diagonal band of Broca and the septal nuclei to the hippocampal formation (11–14).

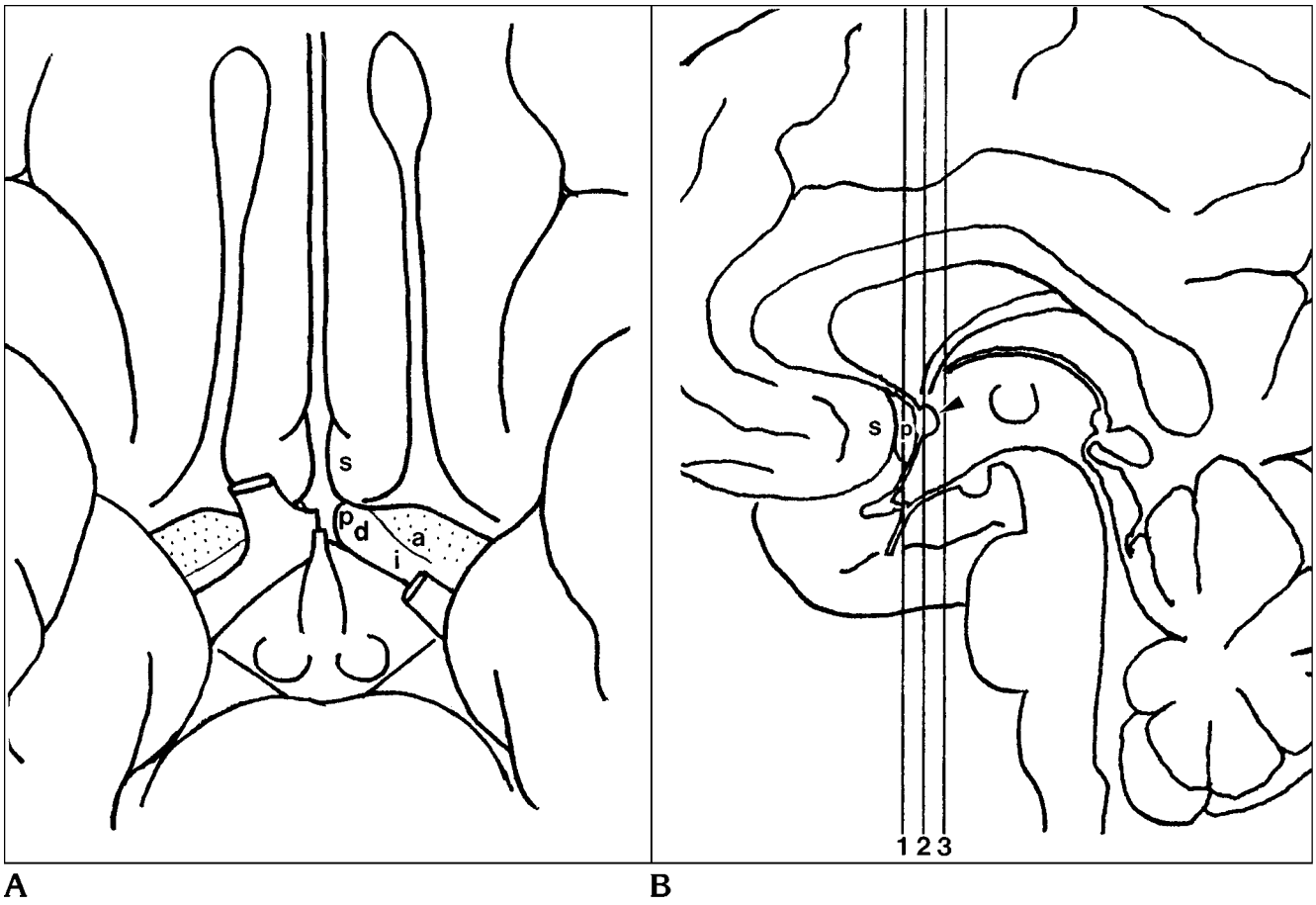

Fig 1. Surface anatomy of the basal forebrain.

A, Schematic drawing viewed from the bottom. The substantia innominata (*i*) and the diagonal gyrus (*d*) are in the posterior part of the anterior perforated substance (*a*). The diagonal gyrus is on the posterolateral aspect of the paraterminal gyrus (*p*), which is located posterior to the subcallosal area (*s*).

B, Schematic drawing viewed from the medial aspect. The paraterminal gyrus (*p*) is located posterior to the subcallosal area (*s*) and anterior to the anterior commissure (*arrowhead*). Three coronal lines indicate the planes we investigated: *1*, the plane through the paraterminal gyrus (Fig 2); *2*, the plane through the anterior commissure (Fig 3); and *3*, the plane through the columna fornicis (Fig 4).

Materials and Methods

Anatomic Study

After formaldehyde fixation and paraffin embedding, contiguous coronal sections of two adult human brains (73-year-old female and 78-year-old male) were obtained. Section thickness was 26 μm, and a combination of Weigert's myelin and Nissl's stains was used.

MR Study

Included in this study were 22 patients with probable Alzheimer disease diagnosed by National Institute of Neurological and Communicative Disorders and Stroke/Alzheimer's Disease and Related Disorders Association criteria (15) (7 male and 15 female patients), 58 to 76 years of age (mean age, 66.9 years), and 14 age-matched patients with other disorders (8 male and 6 female patients), 60 to 75 years of age (mean age, 67.3 years). They were prospectively examined using a 1.5-T superconductive MR unit (Signa Advantage, General Electric, Milwaukee, Wis). Indication for MR imaging in all the control patients was suspicion of mild cerebrovascular occlusive disease. Patients having major neurologic deficits, dementia, memory disturbance, parkinsonism, alcoholism, and any lesions possibly including the basal forebrain were excluded from the control subjects. Patients having tortuous vessels compressing substantia innominata were also excluded. This criterion excluded one control patient (existence of the tortuous right middle cerebral artery compressing the right substantia innominata). The remaining 13 control patients ranged in age from 60 to 75 years (mean age, 67.1 years).

Pulse sequences used were coronal fast spin-echo 3000/102/2 (repetition time/effective echo time/excita-

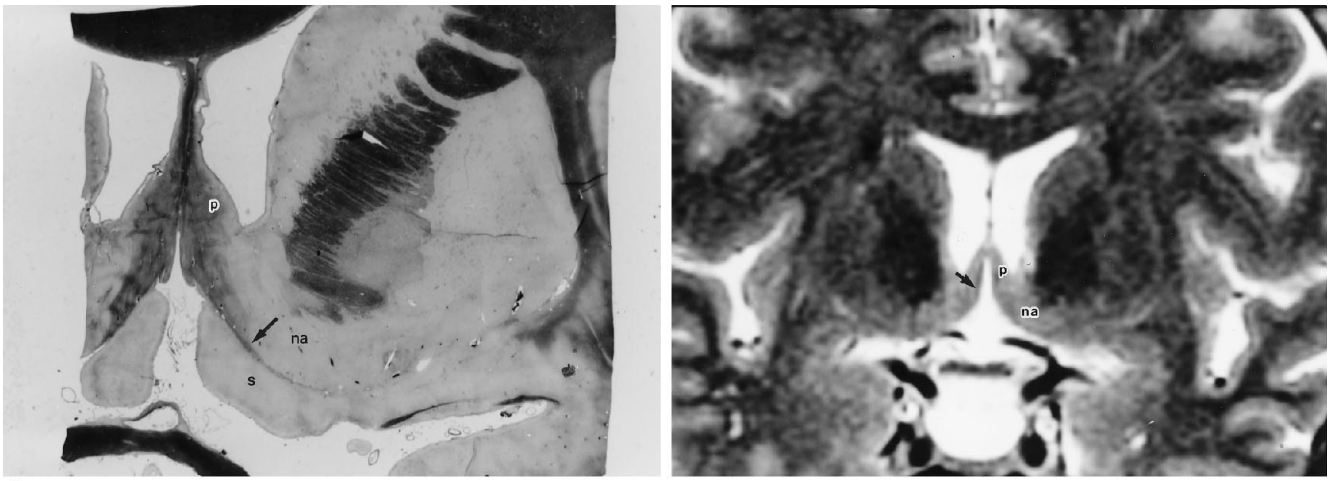

Fig 2. Plane through the paraterminal gyrus (line 1 on Fig 1B).

A, Coronal section of the human specimen from a woman 73 years of age. The posterior border of the subcallosal area (*s*) is shown on the inferomedial surface of the cerebral hemisphere. Myelinated nerve fibers, including the medial olfactory stria and the diagonal band of Broca (*arrow*), are demonstrated between the subcallosal area and the nucleus accumbens septi (*na*). The paraterminal gyrus (*p*) is located superomedial to these structures (Weigert's myelin and Nissl's stains).

B, Corresponding coronal T2-weighted (3000/102) MR image from a control subject (59-year-old woman). The paraterminal gyrus (*p*) and the nucleus accumbens septi (*na*) are identified. A curvilinear structure with white matter signal intensity (*arrow*) probably corresponds to the medial olfactory stria and the diagonal band of Broca.

tions) sequences as T2-weighted images. The echo train length was 16. Section thickness was 3 mm with 1-mm intersection gaps. The matrix size was 256 × 256, and the field of view was 200 mm. These images were obtained in all the patients and control subjects and were perpendicular to the anterior commissure–posterior commissure line. In three control subjects, coronal T1-weighted images were obtained by fast inversion-recovery 2500/34/4 (inversion time, 670) sequences. Section thickness was 3 mm with 1-mm intersection gaps. The data acquisition matrix was 256 × 256, and the field of view was 200 mm.

Balanced and T2-weighted axial images in fast spin-echo sequences (3000/17,102/1) were also obtained in all of the cases. The echo train length was eight. Section thickness was 5 mm with 2 mm intersection gaps. The matrix size was 256 × 192, and the field of view was 220 mm.

The anatomic specimens were used as a guideline to estimate where certain anatomic structures would appear on the MR images, specifically in three contiguous coronal planes: (*a*) one through the paraterminal gyrus, (*b*) one through the anterior commissure, and (*c*) one through the columna fornicis (Fig 1B).

The thickness and signal intensity of the substantia innominata were blindly evaluated by one of the authors (M.S.), and they were compared between patients with Alzheimer disease and control subjects. To measure the thickness, an image analysis program on a workstation of the PACS (picture archiving and communicating system, DataView, General Electric-Yokogawa Medical Systems, Tokyo, Japan) was used. The thickness of the substantia innominata was determined on the coronal T2-weighted image through the anterior commissure. The contrast among the substantia innominata, globus pallidus, and cerebrospinal fluid was carefully optimized on the cathode ray terminal before the measurement. The distance between the lower margin of the low signal area, corresponding to globus pallidus, and the surface of the substantia innominata was measured at the narrowest portion in the middle third of the substantia innominata. The signal intensity of the substantia innominata was visually evaluated on the same images.

Results

In healthy subjects, the substantia innominata was not depicted on the plane through the paraterminal gyrus (Fig 2) but was best visualized on the plane through the anterior commissure (Fig 3). It was also seen on the plane through the columna fornicis (Fig 4). On the section of the specimen through the anterior commissure, the anterior commissure penetrated the globus pallidus, so that the substantia innominata was located not below the anterior commissure but below the subcommissural part of the globus pallidus (Fig 3A). On the T2-weighted image of the corresponding plane, the superior margin of the substantia innominata was readily distinguished from the low signal

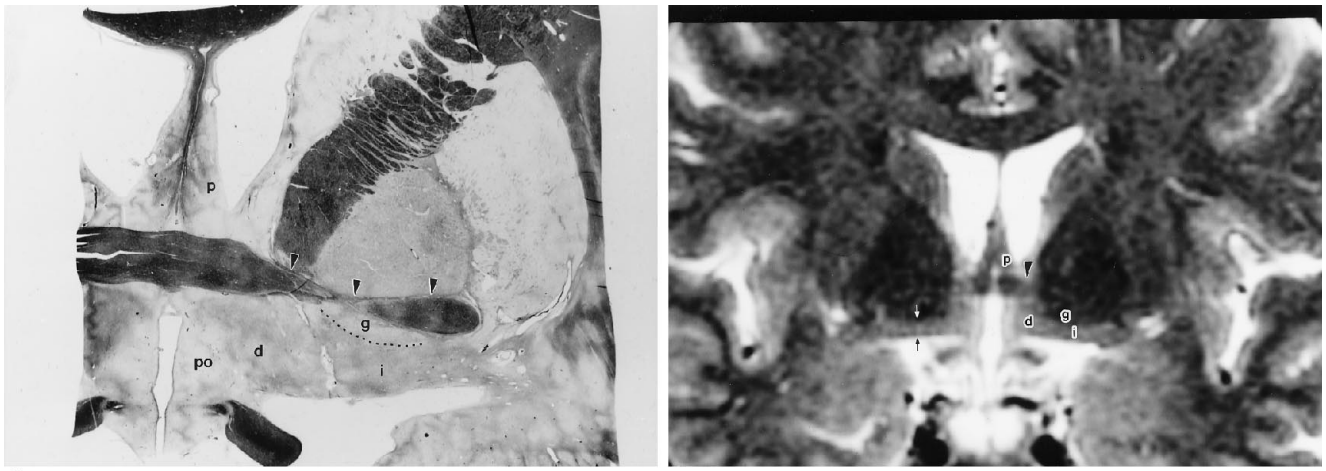

Fig 3. Plane through the anterior commissure (line 2 on Fig 1B).

A, Coronal section of the specimen (73-year-old woman). The substantia innominata (*i*) is identified as a narrow area below the subcommissural part of the globus pallidus (*g*), which is below the anterior commissure (*arrowheads*) penetrating the globus pallidus. The *dotted line* shows the boundary between the globus pallidus and the substantia innominata. The diagonal gyrus (*d*), shown in an L-shaped configuration, is located in the paramedian region. The posterior part of the paraterminal gyrus (*p*) is a median triangular area, superior to the anterior commissure (*arrowheads*). *po* indicates preoptic area (Weigert's myelin and Nissl's stains).

B, Corresponding T2-weighted (3000/102) MR image in a control subject (59-year-old woman). The substantia innominata (*i*), the diagonal gyrus (*d*), and the posterior part of the paraterminal gyrus (*p*) are identified. The substantia innominata is clearly distinguished from the subcommissural part of the globus pallidus (*g*) because of the low signal intensity of the globus pallidus. The substantia innominata and the diagonal gyrus have the signal intensity of the gray matter. The measured portion of the substantia innominata thickness is indicated by *arrows*. The *arrowhead* indicates the anterior commissure.

C, T1-weighted (2500/670/34) MR image in the same control subject as in B. The upper margin of the substantia innominata is not evident.

intensity, which may represent the globus pallidus because of its magnetic susceptibility effect (Fig 3B). It was not possible to distinguish them on T1-weighted images (Fig 3C). Medial and lateral margins of the substantia innominata were not evident on any images. The substantia innominata had the signal intensity of the gray matter on T1- and T2-weighted images. On the plane through the columna fornicis, the substantia innominata was identified as a small triangular substance surrounded by the optic tract, the anterior commissure, the globus pallidus, and the amygdala (Fig 4).

In subjects with Alzheimer disease, T2-weighted images through the anterior commissure (Fig 3B) were used to evaluate the thickness of the substantia innominata. The average thickness of the narrowest portions on the right and left substantia innominatas ranged from 1.3 to 2.6 mm in Alzheimer disease (mean, 2.1 mm; SD, 0.4 mm), and was 2.6 to 3.5 mm (mean, 3.0 mm; SD, 0.4 mm) in the control group. Only three patients with Alzheimer disease had thick substantia innominata in the range of control subjects. The decrease in the thickness was statistically significant in patients with Alzheimer disease ($P < .01$) (Table and Figs 5 and 6). No statistical difference was found between the thickness of right and left substantia innominatas (Table). The signal intensity in the substantia innominata was not altered in any patients.

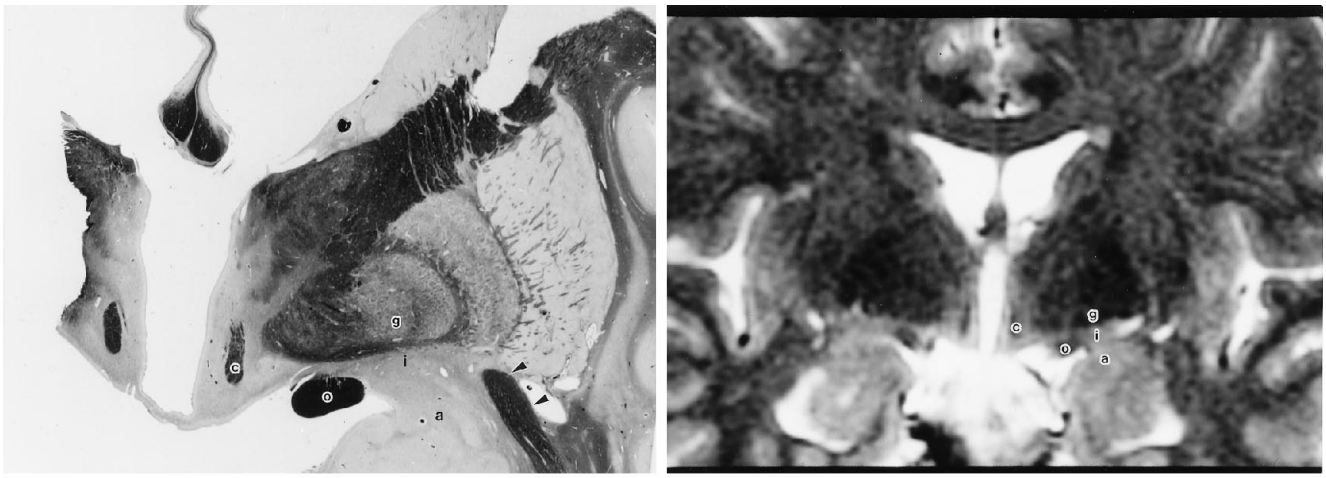

Fig 4. Plane through the columna fornicis (line 3 on Fig 1B).

A, Coronal section of the human brain specimen from a man 78 years of age. The substantia innominata (*i*) is seen as a narrow area surrounded by the optic tract (*o*), the anterior commissure (*arrowheads*), the amygdala (*a*), and the globus pallidus (*g*). The paraterminal gyrus and the diagonal gyrus are not included in this plane. *c* indicates the columna fornicis (Weigert's myelin and Nissl's stains).

B, Corresponding coronal T2-weighted (3000/102) MR image in a control subject (59-year-old woman). The substantia innominata (*i*) is seen as a small area between the optic tract (*o*), the amygdala (*a*), and the globus pallidus (*g*). Its signal intensity is that of the gray matter. *c* indicates the columna fornicis.

Discussion

Recent advances in neuropathology have shown marked neuronal loss of the nucleus basalis of Meynert in the basal forebrain in patients with Alzheimer disease (1, 2). In such cases, diffuse loss of choline acetyltransferase activity in the cerebral cortex is considered to be related to neuronal depletion of the nucleus basalis of Meynert (16–18). Although neuronal loss in other sites, such as the locus ceruleus (19, 20) and the nucleus raphe dorsalis (21), has also been noted, the nucleus basalis of Meynert is believed to be a particularly important site in Alzheimer disease.

Although the nucleus basalis of Meynert has been thoroughly investigated histologically, little attention has been paid in imaging studies. The basal forebrain including the substantia innominata has not been well visualized on computed tomography because of its small size and orientation, which is almost parallel to the axial plane. Even on MR imaging, only brief descriptions by a few authors exists (22–24). Based on our study, the substantia innominata can readily be identified on coronal T2-weighted images as a region of gray matter signal intensity. Because the substantia innominata contains not only the nucleus basalis of Meynert but also nerve tracts, such as the diagonal band of Broca and other amygdalofugal fibers, atrophy of the substantia innominata does not necessarily indicate neuronal loss of the nucleus basalis of Meynert. However, we may at least suggest that the substantia innominata has some role in the process of Alzheimer disease.

Thickness of the substantia innominata in Alzheimer disease

	Thickness, mm		
	Right	Left	Average
Alzheimer disease (n = 22)	2.2 ± 0.4	2.1 ± 0.4	2.1 ± 0.4
Control (n = 13)	2.9 ± 0.5	3.1 ± 0.3	3.0 ± 0.4

Note.—Values are mean ± SD.

We used fast spin-echo because it was appropriate for evaluation of the thickness of the substantia innominata in addition to having a short acquisition time. With a conventional spin-echo technique, signal loss of the globus pallidus caused by its magnetic susceptibility effect is significant in elderly patients, particularly in those with Alzheimer disease (25, 26). Therefore, it is possible to underestimate the thickness of the substantia innominata. With the fast spin-echo technique, such signal loss is less prominent (27, 28), but the contrast between the globus pallidus and the substantia innominata is still sufficient to determine the boundary.

A volume measurement of the substantia innominata might be more sensitive than a linear

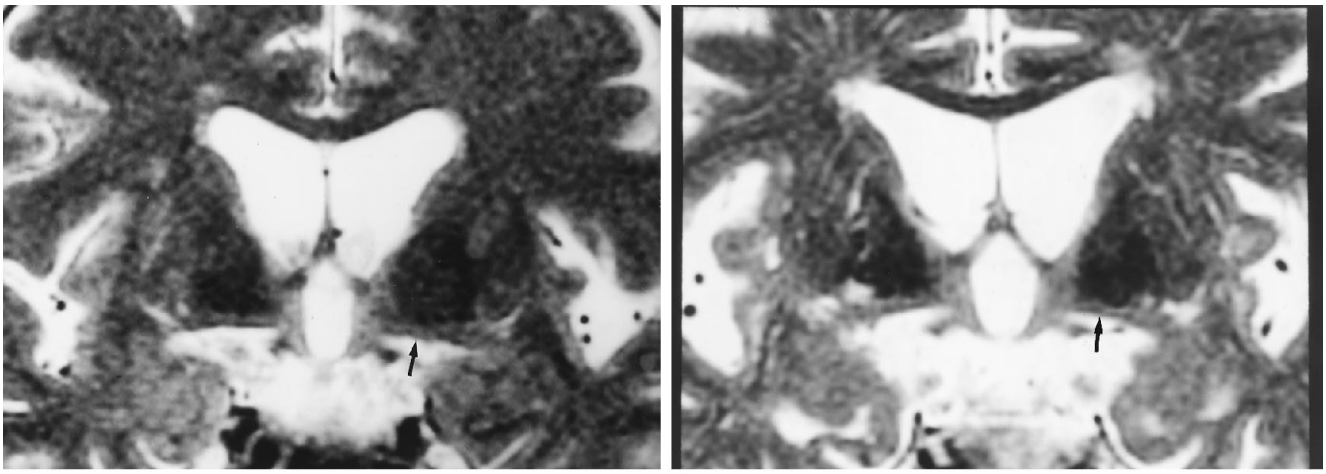

5 6

Fig 5. T2-weighted (3000/102) MR image in a 62-year-old man with Alzheimer disease. The thinning of the substantia innominata is noted (*arrow*).

Fig 6. T2-weighted (3000/102) MR image in a 76-year-old man with Alzheimer disease. The thinning and the concave inferior surface of the substantia innominata are evident (*arrow*).

measurement to evaluate atrophy, but it is difficult, because the anteroposterior and mediolateral margins are not evident. Therefore, measuring the superoinferior dimension of the midportion of the substantia innominata on coronal MR images is probably the only available method. For this method, exact positioning is crucial, because angulation of the scan plane affects the thickness of the substantia innominata. In addition, because it is a very thin structure, higher spatial resolution and a thinner section thickness are also needed to avoid volume averaging.

The value of the thickness of the substantia innominata on an MR scan for differentiating Alzheimer disease from other disorders with dementia remains controversial. Neuronal loss in the nucleus basalis of Meynert is not a specific finding in Alzheimer disease, and we can see it in various other disease processes, such as Parkinson disease (29), parkinsonism-dementia complex of Guam (30), alcoholic Korsakoff disease (29), Creutzfeldt-Jakob disease (31), progressive supranuclear palsy (32), and Pick disease (33). On the other hand, many MR findings in Alzheimer disease have been reported, such as atrophy of the mesial temporal lobe, including the hippocampus and the amygdala (34–36), enlarged interuncal distance (37), and altered signal of the mesial temporal lobe (38). This is a preliminary study, and further studies on the specificity of the MR changes in the substantia innominata and the correlation with other reported MR features in Alzheimer disease are in progress. We believe that morphologic analysis of the substantia innominata should promote further understanding of Alzheimer disease.

Acknowledgments

We gratefully thank K. Tohyama, PhD, DVM, and K. Kumagai (Department of Anatomy, Iwate Medical University) for their kind help in tissue preparation.

References

1. Whitehouse PJ, Price DL, Clark AW, Coyle JT, DeLong MR. Alzheimer's disease: evidence for selective loss of cholinergic neurons in the nucleus basalis. *Ann Neurol* 1981;10:122–126
2. Whitehouse PJ, Price DL, Struble RG, Clark AW, Coyle JT, DeLong MR. Alzheimer's disease and senile dementia: loss of neurons in the basal forebrain. *Science* 1982;215:1237–1234
3. Carpenter MB, Sutin J. *Human Neuroanatomy*. 8th ed. Baltimore: Williams & Wilkins, 1983:612–642
4. Barr ML, Kiernan JA. *The Human Nervous System: An Anatomical Viewpoint*. 5th ed. Philadelphia: Lippincott, 1988:259–274
5. Williams PL, Warwick R, Dyson M, Bannister LH. *Gray's Anatomy*. 37th ed. Edinburgh: Churchill Livingstone, 1989:1028–1039
6. DeArmond SJ, Fusco MM, Dewey MM. *Structure of the Human Brain. A Photographic Atlas*. 3rd ed. New York: Oxford University Press, 1989:136–143
7. Nieuwenhuys R, Voogd J, van Huijzen C. *The Human Central Nervous System. A Synopsis and Atlas*. 2nd ed. New York: Springer, 1981:181–211
8. Hedreen JC, Struble RG, Whitehouse PJ, Price DL. Topography of the magnocellular basal forebrain system in human brain. *J Neuropathol Exp Neurol* 1984;43:1–21
9. Gorry JD. Studies on the comparative anatomy of the ganglion basale of Meynert. *Acta Anat* 1963;55:51–104

10. Andy OJ, Stephan H. The septum in the human brain. *J Comp Neurol* 1968;133:383–410
11. Pearson RCA, Gatter KC, Brodal P, Powell TPS. The projection of the basal nucleus of Meynert upon the neocortex in the monkey. *Brain Res* 1983;259:132–136
12. Mesulam MM, Mufson EJ, Levey AI, Wainer BH. Cholinergic innervation of cortex by the basal forebrain: cytochemistry and cortical connections of the septal area, diagonal band nuclei, nucleus basalis (substantia innominata), and hypothalamus in the rhesus monkey. *J Comp Neurol* 1983;214:170–197
13. Saper CB. Organization of cerebral cortical afferent systems in the rat, I: magnocellular basal nucleus. *J Comp Neurol* 1984;222: 313–342
14. Johnston MV, McKinney M, Coyle JT. Evidence for a cholinergic projection to neocortex from neurons in basal forebrain. *Neurobiology* 1979;76:5392–5396
15. McKhann G, Drachman D, Folstein M, Katzman R, Price D, Stadlan EM. Clinical diagnosis of Alzheimer's disease: report of the NINCDS-ADRDA work group under the auspices of the Department of Health and Human Services Task Force on Alzheimer's disease. *Neurology* 1984;34:939–944
16. Rossor MN, Garrett NJ, Johnson AL, Mountjoy CQ, Roth M, Iversen LL. A post-mortem study of the cholinergic and GABA systems in senile dementia. *Brain* 1982;105:313–330
17. White P, Hiley CR, Goodhardt MJ, et al. Neocortical cholinergic neurons in elderly people. *Lancet* 1977;I:668–671
18. Davies P, Maloney AJF. Selective loss of central cholinergic neurons in Alzheimer's disease. *Lancet* 1976;II:1403
19. Mann DM, Yates PO, Hawkes J. The noradrenergic system in Alzheimer and multiinfarct dementias. *J Neurol Neurosurg Psychiatry* 1982;45:113–119
20. Iversen LL, Rossor MN, Reynolds GP, et al. Loss of pigmented dopamine-b-hydroxylase positive cells from locus coeruleus in senile dementia of Alzheimer's type. *Neurosci Lett* 1983;39:95–100
21. Yamamoto T, Hirano A. Nucleus raphe dorsalis in Alzheimer's disease: neurofibrillary tangles and loss of large neurons. *Ann Neurol* 1985;17:573–577
22. Naidich TP, Daniels DL, Pech P, Haughton VM, Williams A, Pojunas K. Anterior commissure: anatomic-MR correlation and use as a landmark in three orthogonal planes. *Radiology* 1986;158:421–429
23. Baulac M, Vitte E, Dormont D, et al. The limbic system: identification of its structures on brain slices. In: Gouaze A, Salamon G, eds. *Brain Anatomy and Magnetic Resonance Imaging*. Berlin: Springer, 1988:140–149
24. Tamraz JC, Iba Zizen MT, Cabanis EA. Magnetic resonance imaging of the eyes and the optic pathways. In: Gouaze A, Salamon G, eds. *Brain Anatomy and Magnetic Resonance Imaging*. Berlin: Springer, 1988:71–83
25. Schenker C, Meier D, Wichmann W, Boesiger P, Valavanis A. Age distribution and iron dependency of the T2 relaxation time in the globus pallidus and putamen. *Neuroradiology* 1993;35:119–124
26. Bartzokis G, Sultzer D, Mintz J, et al. In vivo evaluation of brain iron in Alzheimer's disease and normal subjects using MRI. *Biol Psychiatry* 1994;35:480–487
27. Listerud J, Einstein S, Outwater E, Kressel HY. First principles of fast spin echo. *Magn Reson Q* 1992;8:199–224
28. Constable RT, Anderson AW, Zhong J, Gore JC. Factors influencing contrast in fast spin-echo MR imaging. *Magn Reson Imaging* 1992;10:497–511
29. Arendt T, Bigl V, Arendt A, Tennstedt A. Loss of neurons in the nucleus basalis of Meynert in Alzheimer's disease, paralysis agitans and Korsakoff's disease. *Acta Neuropathol (Berl)* 1983;61: 101–108
30. Nakano I, Hirano A. Neuron loss in the nucleus basalis of Meynert of parkinsonism-dementia complex of Guam. *Ann Neurol* 1983; 13:87–91
31. Arendt T, Bigl V, Arendt A. Neurone loss in the nucleus basalis of Meynert in Creutzfeldt-Jakob disease. *Acta Neuropathol (Berl)* 1984;65:85–88
32. Tagliavini F, Pilleri G, Gemignani F, Lechi A. Neuronal loss in the basal nucleus of Meynert in progressive supranuclear palsy. *Acta Neuropathol (Berl)* 1983;61:157–160
33. Uhl GR, Hilt DC, Hedreen JC, Whitehouse PJ, Price DL. Pick's disease (lobar sclerosis): depletion of neurons in the nucleus basalis of Meynert. *Neurology* 1983;33:1470–1473
34. George AE, de Leon MJ, Stylopoulos LA, et al. CT diagnostic features of Alzheimer disease: importance of the choroidal/hippocampal fissure complex. *AJNR Am J Neuroradiol* 1990;11: 101–107
35. De Leon MJ, Golomb J, George AE, et al. The radiologic prediction of Alzheimer disease: the atrophic hippocampal formation. *AJNR Am J Neuroradiol* 1993;14:897–906
36. Lehericy S, Baulac M, Chiras J, et al. Amygdalohippocampal MR volume measurements in the early stages of Alzheimer disease. *AJNR Am J Neuroradiol* 1994;15:929–937
37. Dahlbeck SW, McCluney KW, Yeakley JW, Fenstermacher MJ, Bonmati C, Van Horn III G. The interuncal distance: a new MR measurement for the hippocampal atrophy of Alzheimer disease. *AJNR Am J Neuroradiol* 1991;12:931–932
38. Kirsch SJ, Jacobs RW, Butcher LL, Beatty J. Prolongation of magnetic resonance T2 time in hippocampus of human patients marks the presence and severity of Alzheimer's disease. *Neurosci Lett* 1992;134:187–190

Please see the commentary on page 2008 in this issue.